

Immortalized human brain endothelial cells and flow-based vascular modeling: a marriage of convenience for rational neurovascular studies

Luca Cucullo^{1,2}, Pierre-Olivier Couraud^{3,4,5,6}, Babette Weksler^{4,7}, Ignacio-Andres Romero⁸, Mohammed Hossain^{1,2}, Edward Rapp⁹ and Damir Janigro^{1,2,10}

¹Division of Cerebrovascular Research, Cleveland Clinic Lerner College of Medicine, Cleveland, Ohio, USA;

²Department of Neurosurgery, Cleveland Clinic Lerner College of Medicine, Cleveland, Ohio, USA;

³Department of Cell Biology, Institut Cochin, Paris, France; ⁴Inserm, U567, Paris, France; ⁵CNRS, UMR 8104, Paris, France; ⁶Université Paris 5, Faculté de Médecine René Descartes, UM 3, Paris, France; ⁷Department of Medicine, Weill Medical College, New York, New York, USA; ⁸Department of Biological Sciences, The Open University, Milton Keynes, UK; ⁹Flocel Inc., Cleveland, Ohio, USA; ¹⁰Department of Molecular Medicine, Cleveland Clinic Lerner College of Medicine, Cleveland, Ohio, USA

In evaluating drugs that enter or are excluded from the brain, novel pharmaceutical strategies are needed. For this reason, we have developed a humanized Dynamic *In vitro* Blood–Brain Barrier model (hDIV-BBB) based on a novel human brain vascular endothelial cell line (HCMEC/D3), which closely mimics the BBB *in vivo*. In this system, HCMEC/D3 was grown in the lumen of hollow microporous fibers and exposed to a physiological pulsatile flow. Comparison with well-established humanized DIV-BBB models (based on human brain and non-brain vascular endothelial cells co-cultured with abluminal astrocytes) demonstrated that HCMEC/D3 cells cultured under flow conditions maintain *in vitro* physiological permeability barrier properties of the BBB *in situ* even in the absence of abluminal astrocytes. Measurements of glucose metabolism demonstrated that HCMEC/D3 cells retain an aerobic metabolic pathway. Permeability to sucrose and two relevant central nervous system drugs showed that the HCMEC/D3 cells grown under dynamic conditions closely mimic the physiological permeability properties of the BBB *in situ* (slope = 0.93). Osmotic disruption of the BBB was also successfully achieved. Peak BBB opening in the DIV-BBB lasted from 20 to 30 mins and was completely reversible. Furthermore, the sequence of flow cessation/reperfusion in the presence of leukocytes led to BBB failure as demonstrated by a biphasic decrease in transendothelial electrical resistance. Additionally, BBB failure was paralleled by the intraluminal release of proinflammatory factors (interleukin-6 and interleukin-1 β) and matrix metalloproteinase-9 (MMP-9). Pretreatment with ibuprofen (0.125 mmol/L) prevented BBB failure by decreasing the inflammatory response after flow cessation/reperfusion.

Journal of Cerebral Blood Flow & Metabolism (2008) 28, 312–328; doi:10.1038/sj.jcbfm.9600525; published online 4 July 2007

Keywords: drug delivery; drug discovery; drug resistance; pharmacodynamic; shear stress

Introduction

The concept of a ‘neurovascular unit’ has reached deserved prominence in basic and clinical neuroscience. Understanding the neurobiology of human disease requires simultaneous studies of various cell types (e.g., neurons, endothelium, glia, and white blood cells) as well as fluid phase factors (adhesion molecules, cytokines, proinflammatory factors, and intravascular shearing forces). The blood–brain barrier (BBB) exemplifies the importance of this recent approach to neuroscience. Loss of BBB structural integrity and function plays a

Correspondence: Dr D Janigro, Department of Cerebrovascular Research, Cleveland Clinic Foundation NB-20 LRI 9500 Euclid Ave, Cleveland, Ohio 44195, USA. E-mail: janigrd@ccf.org

This work was supported by Alternative Research Development Foundation (ARDF) and Philip Morris USA and Philip Morris International external research awards to Dr Luca Cucullo and was also supported by NIH-2RO1 HL51614, NIH-RO1 NS43284 NIH-RO1 NS38195 and Philip Morris USA and Philip Morris International external research awards to Damir Janigro.

Received 18 December 2006; revised 17 May 2007; accepted 22 May 2007; published online 4 July 2007

pivotal role in the pathogenesis of many diseases of the central nervous system (CNS). The BBB is altered in many clinical settings including brain trauma (Unterberg *et al*, 2004), focal brain ischemia (Latour *et al*, 2004), meningitis (van der *et al*, 2004), brain tumor (Lee *et al*, 2006), stroke (Cipolla *et al*, 2004), inflammation (Stamatovic *et al*, 2006), Alzheimer's disease (Kalaria, 1992), and multiple sclerosis (Minagar and Alexander, 2003). In ischemic brain injury, matrix metalloproteinases (MMPs) contribute to the disruption of the BBB leading to vasogenic edema, and to the influx of leukocytes into the CNS (Gasche *et al*, 2006). In contrast, it has been recently demonstrated that HIV penetration into the brain does not involve the disruption of the BBB. Instead, immune cells, viruses, and viral proteins probably activate brain endothelial cells and enable their own passage across the BBB by way of highly regulated processes such as diapedesis and adsorptive endocytosis (Banks *et al*, 2006). Therefore, understanding how the BBB might be affected by various pathogenic or drug factors holds significant promises for the development of novel pharmacological therapies.

Although the failure of the BBB plays a primary role in the pathogenesis of many CNS diseases, normal BBB structural and functional integrity (which maintains the homeostasis of the CNS environment (Abbott, 2002)) may severely hinder the delivery of drugs into the brain. The presence of active carrier-mediated transport of substrates from the brain to the blood is, in fact, one of the major features of the BBB. By preventing the passage of drugs that are actively extruded by carriers such as P-glycoprotein and multidrug resistance-associated proteins (a phenomenon known as multidrug resistance), the BBB represents a critical obstacle for the treatment of neurologic diseases (Kubota *et al*, 2006). Developing solutions to augment the minimal ingress through the BBB of these potential CNS drugs is essential to improve neurotherapeutics (Pardridge, 2005).

Given these premises, the development of an *in vitro* model of the human BBB that recapitulates the physiologic features of the BBB *in situ* (including the presence of intraluminal flow such as the dynamic *in vitro* BBB model or DIV-BBB) represents an important improvement over the classical static culture system (Santaguida *et al*, 2006). This model has been further enhanced by using primary brain endothelial and glial cells from rats (Krizanac-Bengez *et al*, 2003) as well as cells from human brain tissue resected from patients undergoing brain surgery for aneurysm or intractable epilepsy. These technical advances allowed to establish the first human disease-based DIV-BBB capable of mimicking the pathophysiological properties of its *in vivo* counterpart (Cucullo *et al*, 2007).

The major obstacle toward the development of humanized models has been the difficulty of isolating primary brain endothelial and glial cells,

which not only are difficult to obtain in quantity, but also have to be freshly isolated each time before use. Given these technical difficulties, we decided to turn to an immortalized human brain microvessel endothelial cell line (HCMEC/D3) (Weksler *et al*, 2005), which we show in this report provides an excellent alternative to primary cells especially when cultured under dynamic (flow-based) conditions. This cell line expresses specific brain endothelial properties, cell surface adhesion molecules, and junctional markers, and does not require the presence of abluminal glial cells to form a physiological as well as anatomical BBB (Weksler *et al*, 2005). Because of their stable properties and indefinite growth potential, HCMEC/D3 cells, unlike primary brain microvascular endothelial cells (HBMECs), provide a long-lasting source of human brain endothelial cells.

In this report, we have measured numerous critical parameters to determine if combining the DIV-BBB technology with HCMEC/D3 cells provided a system that could be reliably used to assess the permeability of CNS drugs and to act as a paradigm to study the functional biology of the BBB. For example, we used HCMEC/D3 cells grown as a differentiated monolayer in the DIV-BBB to evaluate the efficacy of currently used clinical protocols such as the osmotic opening of the BBB (which is used to enhance the passage of chemotherapeutic agents for the treatment of brain tumors) (Rapoport, 2000). In addition, we performed experiments to assess if HCMEC/D3 mimics the *in vivo* physiological responses to an ischemic insult (i.e., the BBB failure after inflammation). This was assessed by imposing flow cessation/reperfusion in the presence of human white blood cells (WBCs).

Materials and methods

Cell Culture

Human brain microvascular endothelial cells (cat. no. 6100), human umbilical vein endothelial cells (HUVECs, cat. no. 8000), and human astrocytes (HAs, cat. no. 1800) were purchased from ScienCell Research Laboratories (San Diego, CA, USA). AVM-ECs were isolated from arteriovenous malformations surgically removed from patients. Human brain microvascular endothelial cell, HUVEC, and AVM-EC were initially expanded in 75 cm² flasks precoated with fibronectin (3 µg/cm²) with the appropriate growth medium consisting of 500 mL of basal medium, 25 mL of fetal bovine serum (ScienCell Research Laboratories, cat. no. 0025), 5 mL of endothelial cell growth supplement (cat. no.; 1052), 100 U/mL penicillin G sodium, and 100 µg/mL streptomycin sulfate.

In addition, we used a novel immortalized human brain microvessel endothelial cell line HCMEC/D3, which retains the morphological characteristics of primary brain endothelial cells and expresses specific brain endothelial markers and cell surface adhesion molecules (Weksler *et al*, 2005). HCMEC/D3 was grown in 75 cm² flasks

precoated with $5 \mu\text{g}/\text{cm}^2$ of rat tail collagen type I (BD Biosciences, cat. no. 354236) in EGM-2 medium (Cambrex, cat. no. CC-4176). HAs were grown in poly-D-lysine precoated flasks ($3 \mu\text{g}/\text{cm}^2$ in Dulbecco's modified essential medium (DMEM-F12) supplemented with 2 mmol glutamine, 5% fetal bovine serum, 100 U of penicillin G sodium per mL, and $100 \mu\text{g}$ of streptomycin sulfate per mL). All cells were maintained at 37°C in humidified air with 5% CO_2 . Cellular growth was monitored every day by inspection using phase-contrast microscopy.

Dynamic *In vitro* Blood–Brain Barrier Setup

The DIV-BBB modules used for the experiments described herein were purchased from Spectrum (cat. no. 400-025, Spectrum Laboratories Inc., Rancho Dominguez, CA, USA). Each module consists of a bundle of 50 hollow polypropylene fibers embedded in a clear plastic chamber that provides an accessible space around the fibers (Figure 1A). Cells are seeded inside the hollow fibers (see below). The porous walls of the hollow fibers allow gas and nutrient exchange between the luminal and the abluminal (extracellular space, ECS) compartments, but do not permit the passage of cells between the two compartments. Both luminal and abluminal areas are accessible by ports that connect to a circuit containing a medium reservoir and a pulsatile pump apparatus (Complete CellMax[®] Quad, cat. no. CMQUAD-C, Spectrum Labora-

tories Inc.). Gaseous exchange (O_2 and CO_2) occurs through the gas-permeable silicone tubing that connects the DIV-BBB cartridge and the medium reservoir (Figure 1A). Four electrodes are positioned in the cartridge, one pair in the luminal and one pair in the abluminal compartments that connect to a computerized monitoring system, which allows for real-time measurements of transendothelial electrical resistance (TEER). The pulsatile pump circulates the medium through the lumen of the artificial capillaries. Nutrients are exchanged between lumen and ECS by diffusion through the $0.5 \mu\text{m}$ transcapillary pores. The pump can be adjusted to produce flow of medium ranging from 1 to 50 ml/min (corresponding to shear stress levels of approximately 1 to 200 dyn/cm^2). The entire apparatus is placed inside a water-jacketed incubator at 37°C with 5% CO for optimal culture conditions.

The lumens of the hollow fibers were precoated with fibronectin ($3 \mu\text{g}/\text{cm}^2$) for HBMEC, HUVEC, and AVM-EC or with $5 \mu\text{g}/\text{cm}^2$ of rat tail collagen type I for HCMEC/D3 to enhance cell attachment and proliferation. The abluminal side of the fibers was precoated with poly-D-lysine ($3 \mu\text{g}/\text{cm}^2$) to improve HA adhesion.

Human endothelial cells were seeded intraluminally inside the fibers ($\approx 4 \times 10^6$ /cartridge) and allowed to expand for 14 days in the presence of astrocytes ($\approx 6 \times 10^6$ /cartridge) placed in the abluminal compartment for HBMEC-, HUVEC-, and AVM-EC-based models or without astrocytes for HCMEC/D3 models. To facilitate cell adhesion, we used an initial flow rate of 1 mL/min for

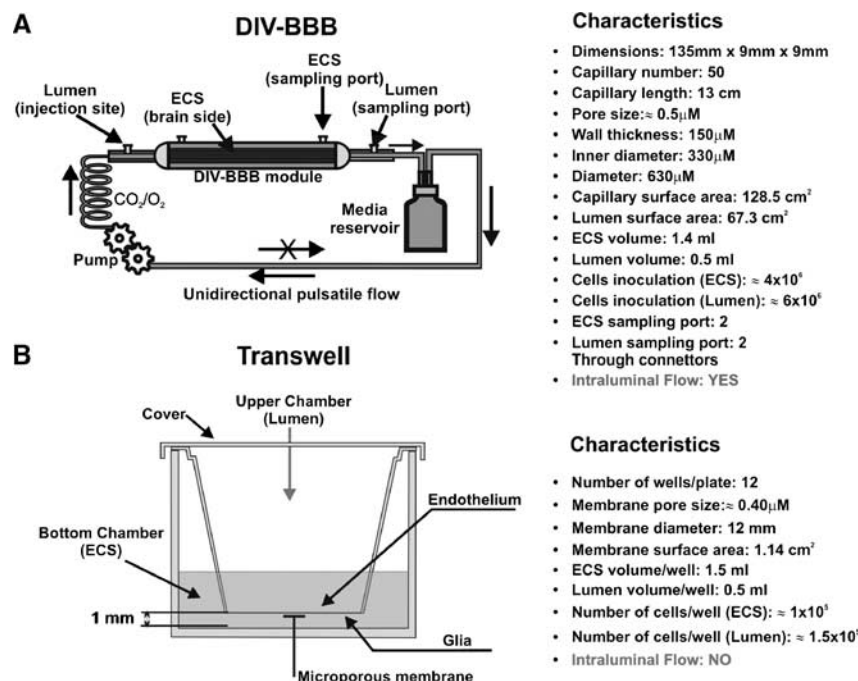


Figure 1 Diagrammatic representation of the DIV-BBB and Transwell systems. (A) A bundle of porous polypropylene hollow fibers is suspended in the DIV-BBB chamber. Note that the hollow fibers are in continuity with a medium source through a flow path consisting of gas-permeable silicon tubing. Two three-way stopcocks positioned on either side of the module regulate the access to the luminal compartment. Detailed dimensional and functional characteristics are shown in the table. (B) The Transwell system consists of endothelial cells grown on microporous membranes, whereas astrocytes are seeded on the underside of the same membrane and release soluble factors, which preserve some of the BBB properties. This system allows for study of bidirectional transport across the BBB. See adjacent table for more details.

the initial 48 h after cell inoculation. The flow rate was then increased to a steady-state level of 4 mL/min (i.e., 4 dyn/cm²). Medium samples from the luminal and abluminal compartments were taken every 2 days and processed to assess for glucose consumption and lactate production.

Transwell Systems

Cells were co-cultured using sets of 12-well Transwell-Clear Polyester Membrane plates (Costar cat. no. 3460), which feature a vertical side-by-side diffusion system through a thin, microscopically transparent polyester membrane of 12 mm diameter and 0.4 μm pore size mounted on a double chamber (Figure 1B). The same coating materials were utilized as in the DIV-BBB to enhance cell attachment. Human endothelial cells (HCMEC/D3, HBMEC, HUVEC, and AVM-EC) were seeded on the top side of the membrane and allowed to establish themselves for 3 days. Human astrocytes were then seeded on the underside of the filter (co-cultures only). The number of cells seeded ranged from 1 × 10⁵ for human endothelial cells to 1.5 × 10⁵ for human astrocytes. Transendothelial electrical resistance was monitored approximately every 2 days beginning at ‘day 1’ of co-culture. The equipment for measuring TEER consisted of a tissue resistance measurement chamber (Endohm chamber, WPI), which provides a reproducible electrical resistance measurement of endothelial tissue culture cups. In conjunction with TEER monitoring, the integrity of the endothelial monolayer was directly assessed by inspection using phase-contrast microscopy (data not shown).

Cell Metabolism: Lactate Production and Glucose Consumption

In conjunction with TEER monitoring, depletion of the main carbohydrate component of the growth medium (glucose) and accumulation of metabolically produced lactic acid were used as indicators of cell growth and the assessment of a viable *in vitro* BBB (Cucullo *et al*, 2007; Santaguída *et al*, 2006). Both the luminal and abluminal compartments (in both DIV-BBB and Transwell) were sampled at 2-day intervals. The calculations for glucose consumption (mg/day) and lactate production rates (mg/day) herein reported were based on medium replacement, volume of non-replaced medium and previous values. Glucose consumption rate was calculated based on the concentration of glucose in fresh and non-replaced medium in the system, according to the following equation:

$$\frac{(V_n \times G_n) + (V_o \times G_p) - (V_t \times G_c)}{T_c - T_p} \quad (1)$$

where *V* represents added volumes of medium (mL), *G* is the glucose concentration (mg/mL), *T* is the time of sampling (in fractions of days), ‘*c*’ and ‘*p*’ indicate the current, and the previous samples, respectively), ‘*n*’ represents the fresh (new) medium added after previous sampling, ‘*o*’ corresponds to the old, unreplaced medium,

and ‘*t*’ represents the total volume of medium. Lactate production rate (mg/day) was calculated similarly:

$$\frac{(V_t \times L_c) - (V_n \times L_n) + (V_u \times L_p)}{T_c - T_p} \quad (2)$$

(*L*) refers to the concentration of lactic acid in mg/mL and ‘*u*’ corresponds to the unreplaced volume of media. A dual-channel immobilized oxidase enzyme biochemistry apparatus (YSI 2700 SELECT, YSI Inc., Yellow Springs, OH, USA) was used to measure lactate and glucose in the culture medium. Data obtained with the described equation were then converted to mmol/L per day.

Dynamic *In vitro* Blood–Brain Barrier Transendothelial Electrical Resistance Measurement System

The TEER measurement provides a quick and easy evaluation of the integrity of the BBB (Cucullo *et al*, 2002, 2007; Santaguída *et al*, 2006). We used a newly developed TEER measurement device (Flocel Inc., Cleveland, OH, USA) (Parkinson *et al*, 2003), which utilizes electronic multiplexing to measure multiple cartridges in quick succession and to assess the integrity and viability of tissue culture monolayers and bilayers rapidly and reliably (Figure 1C). The device uses a Universal Serial Bus interface to a PC computer. To sample TEER, the excitation voltage (0.06 V) is applied across the excitation electrodes inserted in each cartridge. The microcontroller computes the resistivity and capacitance per cm² of the barrier from physical parameters. The values of capacitance are calculated by comparison of the voltage and current waveforms. The delay from peak to peak of the two waveforms is proportional to the capacitance value, which is expressed as archtension. Transendothelial electrical resistance was measured continuously from the initial setup throughout the course of each experiment.

Drug Permeability: Uptake of [¹⁴C]Phenytoin, [¹⁴C]Diazepam, and [³H]Sucrose

Concentrated Boluses (0.5 mL each) of the radioactive tracers [¹⁴C]phenytoin (PerkinElmer, Boston, MA, USA; cat. no. NEC-246), [¹⁴C]diazepam (Amersham, Piscataway, NJ, USA; cat. no. CFA-591), and [³H]sucrose (Amersham, cat. no. TRA-332) were injected upstream (before the capillary cartridge) into the lumen and the diffusion of each substance from luminal into the ECS was monitored over time while maintaining a 1 mL/min intraluminal perfusion rate. A total of 1 μCi per compound was used. The reduction of flow rate from 4 to 1 mL/min (equivalent to a reduction of shear stress from 4 to 1 dyn/cm²) for a short period of time (1 h) does not affect BBB integrity. This has been previously demonstrated by our group (Desai *et al*, 2002) and by others (Mashour and Boock, 1999).

[¹⁴C]Phenytoin, [¹⁴C]diazepam, and [³H]sucrose were chosen because they are representative of three different classes of compounds. Sucrose is a well-known paracellular marker and its permeability across the BBB has been

acknowledged as a good indicator of BBB integrity. Diazepam is a highly lipophilic antidepressant that transverses the BBB by a mechanism of passive diffusion. Phenytoin is an antiepileptic drug, which is also a substrate for multidrug transport systems such as MDR1.

Samples of culture medium (100 μ L) were taken from the ECS and lumen (Parkinson *et al*, 2003) at time 0 (immediately after the injection of isotope) and at 1, 3, 5, 10, 15, 30, and 60 mins after the injection. Note also that luminal samples were collected downstream of the cartridge (at the point where the medium leaves the capillary to enter the silicon tubing). The medium removed from the ECS was replaced with equal volumes of fresh medium. Samples were then introduced into vials with 4 mL of Ready Protein Beckman scintillation cocktail (Packard Ultima Gold, ECN, Costa Mesa, CA, USA). Radioactivity was counted with an LS 6500 scintillation counter (Beckman Coulter Inc., Fullerton, CA, USA).

Permeability for a given compound was calculated as described elsewhere (Cucullo *et al*, 2007; Davson and Segal, 1996). In brief, the permeability to a specific compound was obtained by using a mathematic formula derived from a differential equation based on Fick's Law reported below:

$$\frac{dM_{ECS}}{dt} = PA(C_{lumen} - C_{ECS}) \quad (3)$$

The equation has been modified based on the characteristics of the DIV-BBB (Stanness *et al*, 1997). In this equation, dM_{ECS} represents the amount of solutes (moles) entering the ECS over time, P is the permeability coefficient, A the surface area of capillaries, C_{lumen} the concentration of solute at the luminal space, and C_{ECS} the concentration of solute in the ECS.

From Fick's law, dividing by the ECS volume (V_{ECS}), we obtain the differential equation for the solute concentration in the ECS:

$$\frac{dC_{ECS}}{dt} = \frac{PA}{V_{ECS}} \times (C_{lumen} - C_{ECS}) \quad (4)$$

where the transfer coefficient K can be expressed as follows:

$$\frac{PA}{V_{ECS}} = K \text{ thus } \frac{dC_{ECS}}{dt} = K(C_{lumen} - C_{ECS}) \quad (5)$$

By integration of this differential equation between the limits of time 0 and t , we obtain $\int_0^t dC_{ECS} = K \int_0^t (C_{lumen} - C_{ECS})$ where the ratio of the line over the area is

$$K = \frac{\int_0^t dC_{ECS}}{\int_0^t (C_{lumen} - C_{ECS})} \quad (6)$$

Now, by solving the defined integral equation, we obtain

$$K = \frac{C_{ECS}(t) - C_{ECS}(0)}{[AUC_{lumen}]_0^t - [AUC_{ECS}]_0^t} \quad (7)$$

where AUC_{lumen} and AUC_{ECS} represent the area under the curve defined by the measured concentrations of the specific compound in the lumen and in the ECS at different time points.

Because K is linked to the permeability as previously described, $\frac{PA}{V_{ECS}} = K$, it is possible to express P as a

function of the surface area of capillaries (A) and the ECS volume (V_{ECS}) as follows: $P = \frac{K \times V_{ECS}}{A}$. At this point, the permeability ' P ' can be calculated because K is a coefficient obtained experimentally and the other parameters are derived from the characteristics of the model and have known values:

$$V_{ECS} = 1.4 \text{ cm}^3; A \text{ (capillary surface area)} = 128.5 \text{ cm}^2$$

To obtain the P value in cm/sec, we have to divide by 60 thus obtaining the final equation specific for the DIV-BBB:

$$P[\text{cm/sec}] = \left[\frac{(C_{ECS}(t) - C_{ECS}(0))}{([AUC_{lumen}]_0^t - [AUC_{ECS}]_0^t)} \right] \times \frac{1.4}{128.5} \times \frac{1}{60} \quad (8)$$

Permeability of the specific compound in 'single pass' experiments was calculated by integrating the area under the ECS and lumen data points (AUC) according to Eq. (8), where $C_{ECS}(t)$ and $C_{ECS}(0)$ are the extraluminal space concentrations of compound x , at time 0 and time (t) = 10 mins. This time interval was chosen to minimize the contribution of drug efflux. Note also that the driving force for drug transfer is not, in these equations, concentration-dependent. In other words, the integral of luminal and ECS values vary only as a function of time. In addition, the diffusion of the drug is independent from the units of measurement used, therefore the dimensions of the drug are canceled out in the equation and the same permeability values (expressed in cm/sec) will be obtained when using molar concentration (mol) or counts per minute (c.p.m.) units (see Eqs 7) and (8)).

BBB Opening by Hyperosmolar Mannitol

Infusion of 2 mL of growth medium containing mannitol (1.6 mol/L) was used to open the BBB in the DIV-BBB apparatus (Rapoport, 2000). The mannitol solution was prepared under sterile conditions and injected intraluminally at a perfusion rate of 2 mL/min (total perfusion time was 30 secs). TEER was monitored during the course of the experiment to assess for BBB failure (=opening) and recovery.

Isolation of White Blood Cells

Blood was collected from healthy donors (in preservative-free heparin or EDTA tubes) and processed within 2 h. Viable mononuclear cells were isolated using an equal volume of Histopaque (HISTOPAQUE®-1077, cat. no. 1077-1, Sigma Aldrich, St Louis, MO, USA). The blood-Histopaque mixture was centrifuged at $400 \times g$ for 30 mins at room temperature with slow deceleration. After centrifugation, the upper layer containing mononuclear cells was aspirated with a Pasteur pipette, transferred into a clean conical centrifuge tube, diluted with 10 mL isotonic phosphate-buffered saline and centrifuged at $250 \times g$ for 10 mins. WBC in the pellet were resuspended in 5 mL of culture medium and counted. White blood cells were injected downstream into the intraluminal space of the DIV-BBB ($\approx 50 \times 10^6$ cells/module).

Flow Cessation and Effects of Reperfusion on Blood–Brain Barrier Function

Four DIV-BBB modules were perfused with WBC (purified mononuclear cell suspensions isolated from healthy volunteers, 1 million/mL, that is total of 35×10^6 WBC/DIV-BBB) in the luminal compartment. A shear stress of 4 dyn/cm² was applied to all the co-cultures. After 24 h, WBCs were injected intraluminally; the pulsatile flow was discontinued for 1 h. The DIV-BBBs were then reperfused under normoxic conditions ($pO_2 \approx 185$ mm Hg) with a normal shear stress of 4 dyn/cm². In parallel, four other DIV-BBB modules were pre-incubated with ibuprofen for 1 h before flow cessation/reperfusion. Ibuprofen was injected into the luminal compartment downstream from the cartridge (5 mL of ibuprofen at 1 mmol/L concentration) and was diluted in a total of 35 mL of circulating medium thus reaching the final concentration of approximately 0.125 mmol/L. This concentration is comparable with peak drug blood levels achieved with oral ibuprofen at doses of approximately 400 mg, where peak concentrations in blood are generally high (20 µg/mL to 0.1 mmol/L). Two other sets of DIV-BBB (four cartridges per set) were used as controls and/or to establish baseline effects ibuprofen on the BBB, respectively. TEER was measured during all the phases of the experiment to monitor the BBB integrity.

Interleukin-6, Interleukin-1 β , and Matrix Metalloproteinase-9 Measurement

Samples (100 µL each) were taken from both the luminal and abluminal compartments at 0, 1, 2, 4, 8, 12, and 24 h after flow cessation/reperfusion. Supernatants of samples obtained from DIV-BBB were stored at -20°C until analysis by enzyme-linked immunosorbent assay (ELISA). Interleukin-6, interleukin-1 β (IL-1 β), and MMP-9 levels in cell culture supernatants were measured by specific ELISA kits according to manufacturer's protocol (MMP-9 ELISA kit, cat. no. QIA56, EMD Biosciences, San Diego, CA, USA; IL-6 and IL-1 β , cat. no. I8428-04 and I7663-14, US Biological Swampscott, MA, USA). Medium samples were removed from both the abluminal fluid and the intraluminal perfusate, centrifuged at $5000 \times g$ for 5 mins, pellets discarded, and supernatants kept frozen until performing ELISA. The biotinylated antibody reagent was added to 96-well ELISA plates after the addition of the specific standards or experimental samples. After washing, the streptavidin–HRP complex was added for 30 mins at room temperature, followed by tetra-methylbenzidine (TMB) and stop solution (1 mol/L sulfuric acid). Cytokine levels were measured by an ELISA plate reader at 450 to 550 nm.

Statistical Analysis

For parametric variables (e.g., TEER levels, glucose consumption, lactate production, cytokines levels), differences between populations were analyzed by ANOVA. *P*-values < 0.05 were considered statistically significant.

Bonferroni analysis was used to account for comparisons of multiple parameters among groups. We used four cartridges/group. On the basis of previous experiments, this number of cartridges provided sufficient power to show statistical significance for positive findings.

Results

Transendothelial Electrical Resistance Measurements

The dynamics of BBB formation and the integrity of the barrier itself were compared in DIV-BBB and Transwell plates by using TEER measurements. We have previously shown that, under flow conditions, endothelial cells grown in a capillary-like support develop a morphology that closely resembles the normal endothelial phenotype *in situ* and permit the development of higher TEER in comparison with a static system (Santaguida *et al*, 2006).

As shown in Figure 2A for three types of endothelial cell systems, the TEER in the DIV-BBB reaches steady state in approximately 2 weeks, whereas the corresponding co-cultures established in Transwell required 1 week (Figure 2B). Transendothelial electrical resistance at the steady state was ≈ 1200 Ohm cm² in all the DIV-BBB with the exception of the HUVEC/HA co-culture-based model (approximately 800 Ohm cm²). No difference was observed in TEER between HCMEC/D3 and HCMEC/D3+HA, thus confirming that this brain vascular endothelium cell line is capable of developing a tight barrier even in the absence of abluminal astrocytes.

By contrast (Figure 2B), Transwell models were characterized by a 15- to 20-fold lower TEER (ranging from 60 to 80 Ohm cm²) in comparison with TEER in DIV-BBB. In addition, after 14 days of co-culture, the Transwell systems developed signs of cellular senescence as reflected by the decreasing TEER values. This was more evident for AVM-EC/HA and HUVEC/HA co-cultures.

Glucose Metabolism

Measurements of glucose consumption and lactate production in the DIV-BBB models (Figure 3) compared to Transwell showed that cells grown under dynamic conditions develop over time a predominantly aerobic metabolism. This same pattern of glucose metabolism was observed in all humanized DIV-BBB models irrespective of different EC types. The HCMEC/D3 models showed similar aerobic metabolic pathways both in the presence and in the absence of abluminal astrocytes. However, showing a marked difference in metabolic behavior from the monoculture condition, when HCMEC/D3 cells were cultured with astrocytes, the metabolic shift from anaerobic to aerobic metabolism occurred immediately. This suggests that the exposure to intraluminal flow in determining the

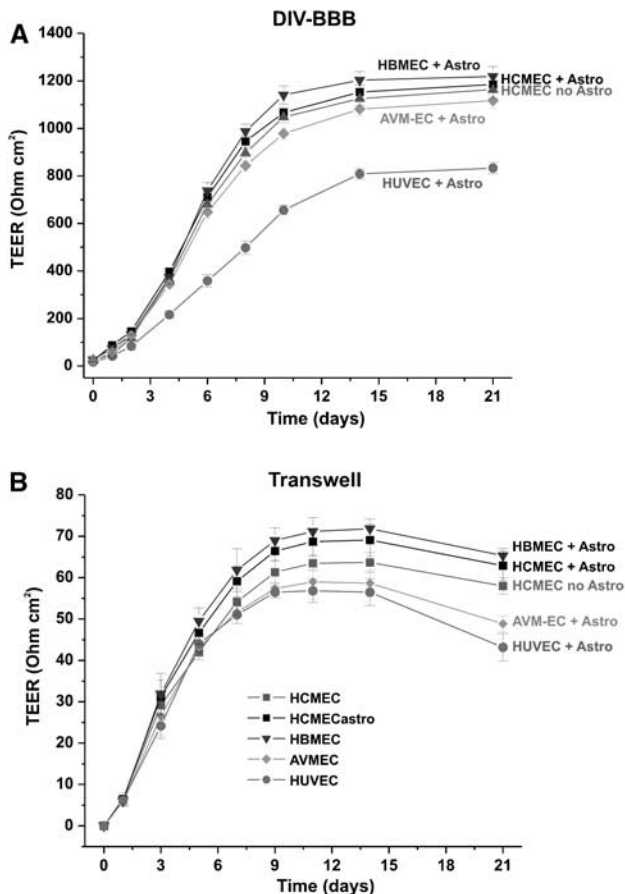


Figure 2 Dynamically grown endothelial cells develop higher TEER in comparison to Transwell. **(A)** Under dynamic conditions, endothelial cells shown a robust differentiation resulting in the development of a far more stringent barrier. This is demonstrated by the high TEER values measured. No difference was observed between HCMEC/D3 alone and HCMEC/D3 co-cultured with abluminal astrocytes. This data confirms that this cell line is capable of developing a tight barrier even in absence of abluminal astrocytes. **(B)** By contrast, TEER peak values measured in parallel Transwell systems were between 15- to 20-fold lower than in DIV-BBB. Note also that in the DIV-BBB the TEER remained stable for the entire length of the experiment (21 days). By contrast, in Transwell, the TEER started to decay after 14 days of culture. Cellular senescence was even more pronounced for non-brain vascular endothelial cell (AVM-EC and HUVEC)-based models.

intracellular bioenergetic pathway (aerobic or anaerobic) is as important as the presence of abluminal astrocyte (Desai *et al*, 2002).

Blood–Brain Barrier Disruption Protocol

Intracarotid infusion of hyperosmolar (1.6 mol/L) mannitol, a cell-impermeable and non-toxic polyalcohol, has been a useful tool for breaching the BBB *in vivo* (Rapoport, 2000). The duration of peak BBB opening induced by mannitol varies from 10 to 30 mins and is completely reversible (Rapoport, 2000).

The DIV-BBBs containing monolayers of cerebral microvascular endothelial cells grown under flow were intraluminally perfused (30 secs) with hyperosmolar mannitol (1.6 mol/L) and TEER was measured to assess real-time changes of BBB integrity (Figure 4). Blood–brain barrier opening was successfully achieved in all the DIV-BBB containing different types of endothelial cells. Similar to the responses achieved *in vivo* (Rapoport, 2000), the duration of peak BBB opening varied from 20 to 30 mins and was completely reversible, thus demonstrating the capacity for DIV-BBB to mimic the BBB's response to exposure to hyperosmolar mannitol *in situ*.

Drug Permeability

A functional BBB model must guarantee selective permeability to molecules based on their oil/water partition coefficient and molecular weight. We performed permeability tests using three different classes of compounds: (1) sucrose (a polar molecule commonly used as paracellular marker); (2) phenytoin (an antiepileptic drug that is a substrate of multidrug transport systems, for example, MDR1); (3) diazepam (a benzodiazepine and a very lipophilic substance that crosses the BBB by passive diffusion). Permeability of each specific compound was calculated by integrating the area under the ECS and lumen data points (AUC) between time 0 and time (t) = 10 mins (min) according to the final Eq. (8) described in the Materials and methods section. The choice of a short specific time interval was necessary to minimize the significance of drug efflux on the permeability calculation. This is more relevant for highly lipophilic drugs where efflux occurs in a short time. A different calculation model may be necessary (Levis *et al*, 2003) to calculate permeability of drugs over a prolonged period of time.

Figure 5A shows the permeability values of [^3H]sucrose measured in HBMEC+HA, HCMEC/D3, HUVEC+HA, and AVM EC+HA DIV-BBB models, where HBMEC+HA has been considered as a standard. Permeability to [^3H]sucrose was $\approx 3 \times 10^{-7}$ cm/sec in HBMEC+HA and HCMEC/D3 DIV-BBB, whereas HUVEC+HA and AVM-EC+HA demonstrated a significantly higher ($P < 0.05$) permeability ($1.18 \times 10^{-6} \pm 0.90$ cm/sec and $1.06 \times 10^{-6} \pm 0.16$ cm/sec, respectively) (Figure 5B). These data are in agreement with the lower TEER values (Figure 1A) measured at steady state in these particular DIV-BBB setups (especially HUVEC+HA).

Permeability measurements to [^{14}C]phenytoin (Figure 6A) showed no significant differences between HBMEC+HA, HCMEC/D3, and AVM EC+HA ($8.43 \times 10^{-6} \pm 1.26$, $9.37 \times 10^{-5} \pm 1.69$, and $1.59 \times 10^{-5} \pm 0.30$ cm/sec, respectively) HUVEC+HA *in vitro* BBB was significantly more permeable ($6.06 \times 10^{-5} \pm 0.33$ cm/sec) to phenytoin ($P < 0.05$) (Figure 6B).

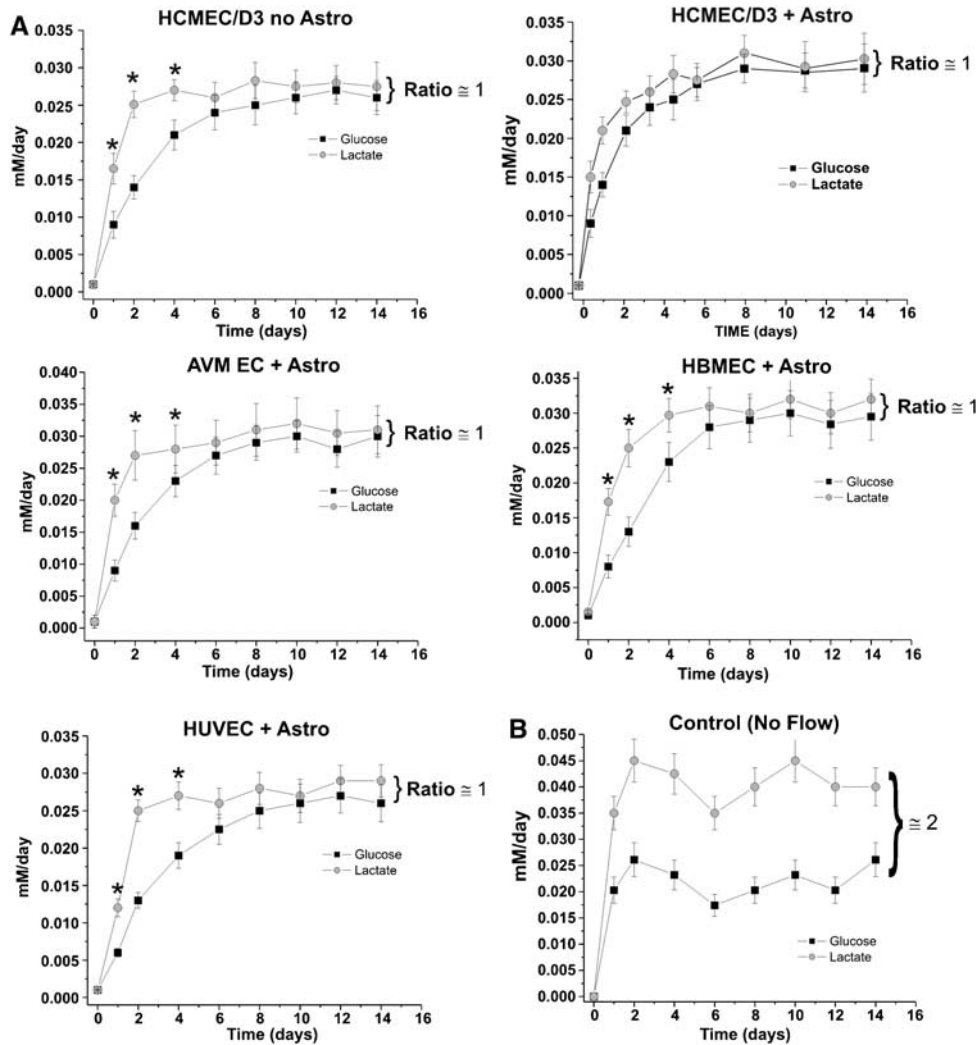


Figure 3 Glucose consumption and lactate production in DIV-BBB versus Transwell. **A** The sharp metabolic increase in glucose consumption (mmol/day) is paralleled by a similar increase in lactate production (ratio between lactate production and glucose consumption was ≈ 1). This suggests that in DIV-BBB cell metabolism is principally aerobic. This was observed in all the DIV-BBB regardless the type of vascular endothelium used. **(B)** By contrast, this phenomenon was not observed under static conditions where the ratio between lactate production and glucose consumption was ≈ 2 , thus suggesting a metabolic pathway primarily anaerobic. Note also that the glucose consumption–lactate production pathway represents the average of the measurement obtained from all the different culture setups used in our experiments. The asterisk ‘*’ indicates glucose/lactate ratios that are significantly different ($P < 0.05$) from 1. Glucose consumption and lactate production values were normalized by the total number of cells ($\approx 2 \times 10^6$).

Finally, permeability measurement to [^{14}C]diazepam (Figure 7A) has shown similar results ($P \approx 2 \times 10^{-3} \text{ cm/sec}$) for all the DIV-BBB (Figure 7B). These data confirm that the DIV-BBB reproduces the physiologic barrier properties of the BBB *in situ*. Note that the ability to form a tight barrier (has been demonstrated by TEER values) affects only the permeability of polar compounds (e.g., sucrose) and becomes less determinant with the increase in the lipophilicity of the substance (phenytoin and diazepam). In this case, the presence of specific efflux carriers can significantly affect the permeability of the substance (Cucullo *et al*, 2007). The relationship between lipophilicity and permeability in the DIV-BBB was similar to that reported by others *in vivo* (Davson and Segal, 1996).

Figure 8A shows the correlation between permeability to sucrose, phenytoin, and diazepam measured in BBB models *in vitro* and published *in vivo* permeability values (Lorberboym *et al*, 2006; Walker *et al*, 1996).

The dashed line indicates the idealized relationship if the *in vivo* data were identical to those *in vitro*. As demonstrated by the slope (S) values, HBMEC+HA ($S=0.92$) and HCMEC/D3 ($S=0.93$) closely reproduced the *in vivo* rank order of permeability and the permeability values of sucrose, phenytoin, and diazepam, whereas AVM-EC+HA ($S=0.80$) and HUVEC+HA ($S=0.78$) demonstrated significantly less accuracy. This appears to be more relevant for polar molecules (such as sucrose) where permeability is principally determined by the BBB

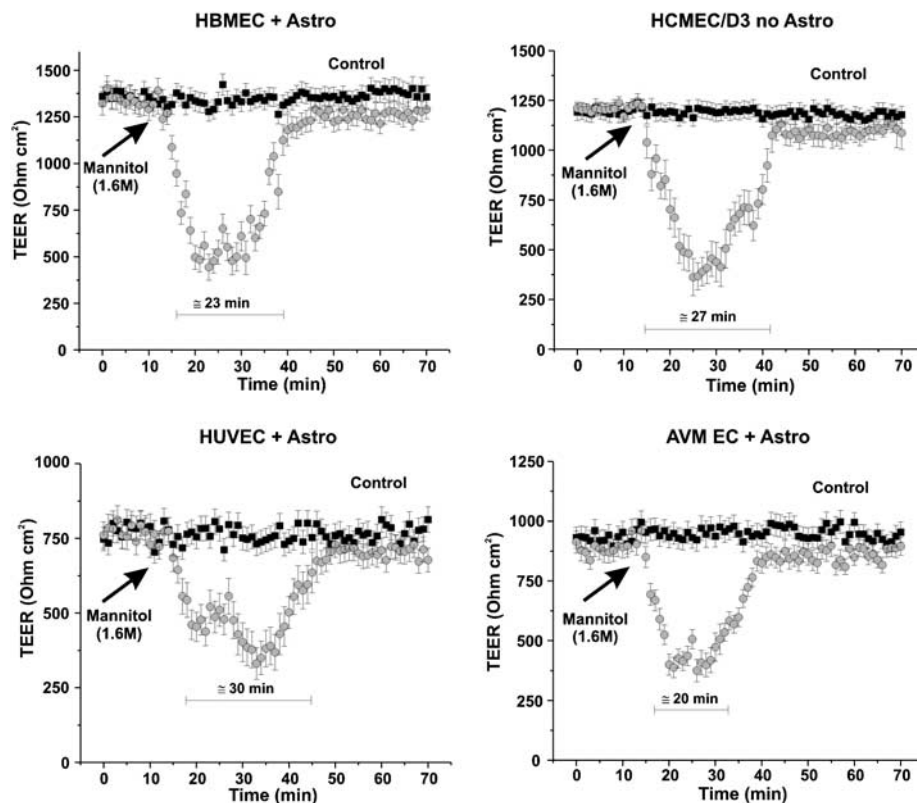


Figure 4 Hyperosmolar opening of the BBB in DIV models. The figures show real-time TEER changes induced by intraluminal perfusion (30 secs) with hyperosmolar mannitol (1.6 mol/L). Note that the duration of peak BBB opening varied from 20 to 30 mins after mannitol perfusion and was completely reversible.

tightness and lack of paracellular pathways. Of importance is the fact that HCMEC/D3 cells grown under dynamic conditions in the absence of abluminal astrocytes demonstrated BBB permeability properties similar to the HBMEC + HA setup.

Figure 8B shows the functional correlation between TEER values and permeability to the paracellular marker, sucrose. High paracellular permeability ($P_{\text{SUCROSE}} < 1 \times 10^{-5}$ cm/sec) is paralleled by TEER values ≤ 800 Ohm cm². Low P_{SUCROSE} values are predicted for Transwell systems in which TEER values are much lower than in corresponding DIV-BBB models (Santaguida *et al*, 2006).

Assessing the Role of Inflammation in BBB Failure

The BBB *in vivo* dynamically responds to events associated with focal ischemia, including flow disturbances, release of reactive oxygen species, and cytokine generation. In particular, the effect of loss of shear stress in presence of WBC under normoglycemic condition causes BBB failure by triggering proinflammatory events such as release of cytokines and MMPs and the activation of WBC (Gasche *et al*, 2006; Krizanac-Bengez *et al*, 2006; Latour *et al*, 2004). Figure 9A shows the baseline TEER values of the four separate control DIV-BBB

modules established with the brain microvascular human cell line HCMEC/D3. These control DIV-BBBs were also exposed to ibuprofen (5.7 μ mol/L final concentration) with and without the presence of circulating WBC. No TEER differences were observed among the controls during customary flow conditions, thus demonstrating that under normal flow conditions BBB integrity was not hampered by treatments with ibuprofen or by the presence of circulating WBC. However, flow cessation (for 1 h) followed by reperfusion, induced a biphasic opening of the BBB as shown in Figure 9B. This is in agreement with *in vivo* observations on patients undergoing ischemic injury (as a consequence of cerebral stroke) who showed breakdown of the BBB (Lorberboym *et al*, 2006) or in rats subjected to middle cerebral artery occlusion, which also showed BBB breakdown (Chen *et al*, 2006). Pretreatment of the DIV-BBB with ibuprofen partially prevented BBB failure and shortened the duration and degree of BBB openings in comparison with untreated modules. These data are in agreement with observation *in vivo* demonstrating that pretreatment with ibuprofen reduced infarct size after induced focal cerebral ischemia (Antezana *et al*, 2003; Cole *et al*, 1993). These data were confirmed by measurements of IL-1 β , IL-6, and MMP-9 release in medium samples (Figure 10). Pretreatment with

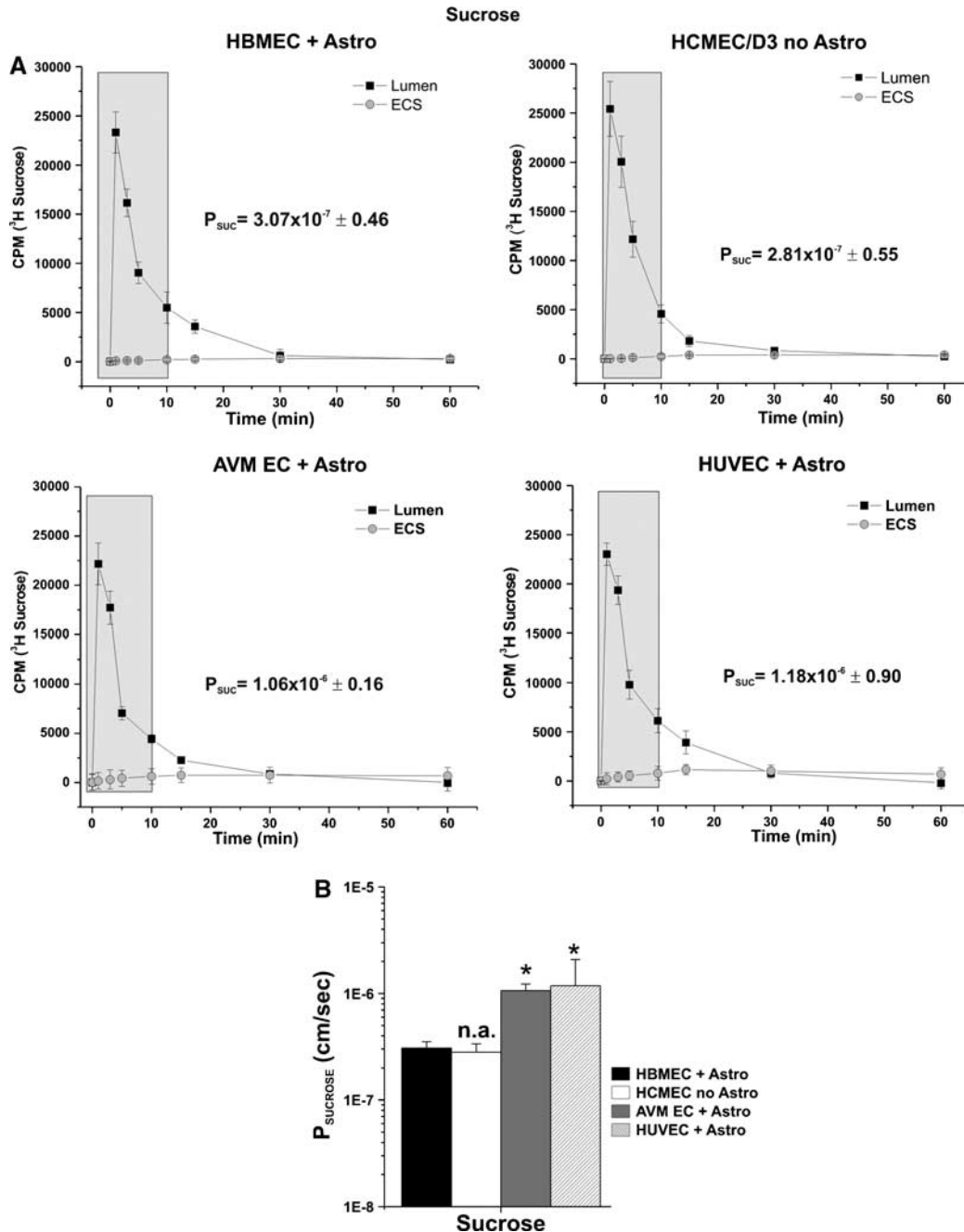


Figure 5 Sucrose permeability: side-by-side comparison of four humanized DIV-BBB models. **(A)** The permeability curves measured in the DIV-BBB are shown. **(B)** Note that permeability to [³H]sucrose was significantly higher in AVM + HA and HUVEC + HA co-cultures setups. Note that all experiments were performed in triplicate; permeability values are expressed in cm/sec ± s.e.m. The asterisk ‘*’ indicates $P < 0.05$. Permeability was measured over a period of time of 10 mins.

ibuprofen significantly reduced the release of proinflammatory cytokines IL-1 β , IL-6, and of MMP-9, all of which have been shown to be involved in the regulation of BBB permeability (Krizanac-Bengez *et al*, 2006; Shigemori *et al*, 2006). It should be noted that HCMEC/D3 cells grown in the DIV-BBB system under flow in the absence of astrocytes are capable of mimicking the physiological behavior of the BBB *in vivo* in response to systemic inflammation.

Discussion

The development of an *in vitro* cell system that mimics the BBB is an important first step in the evaluation of new drug delivery technology across the BBB. Such a system allows rapid screening for (1) identifying brain-specific targeting ligands; (2) screening new experimental drug compounds; (3) testing the efficiency of drug delivery systems;

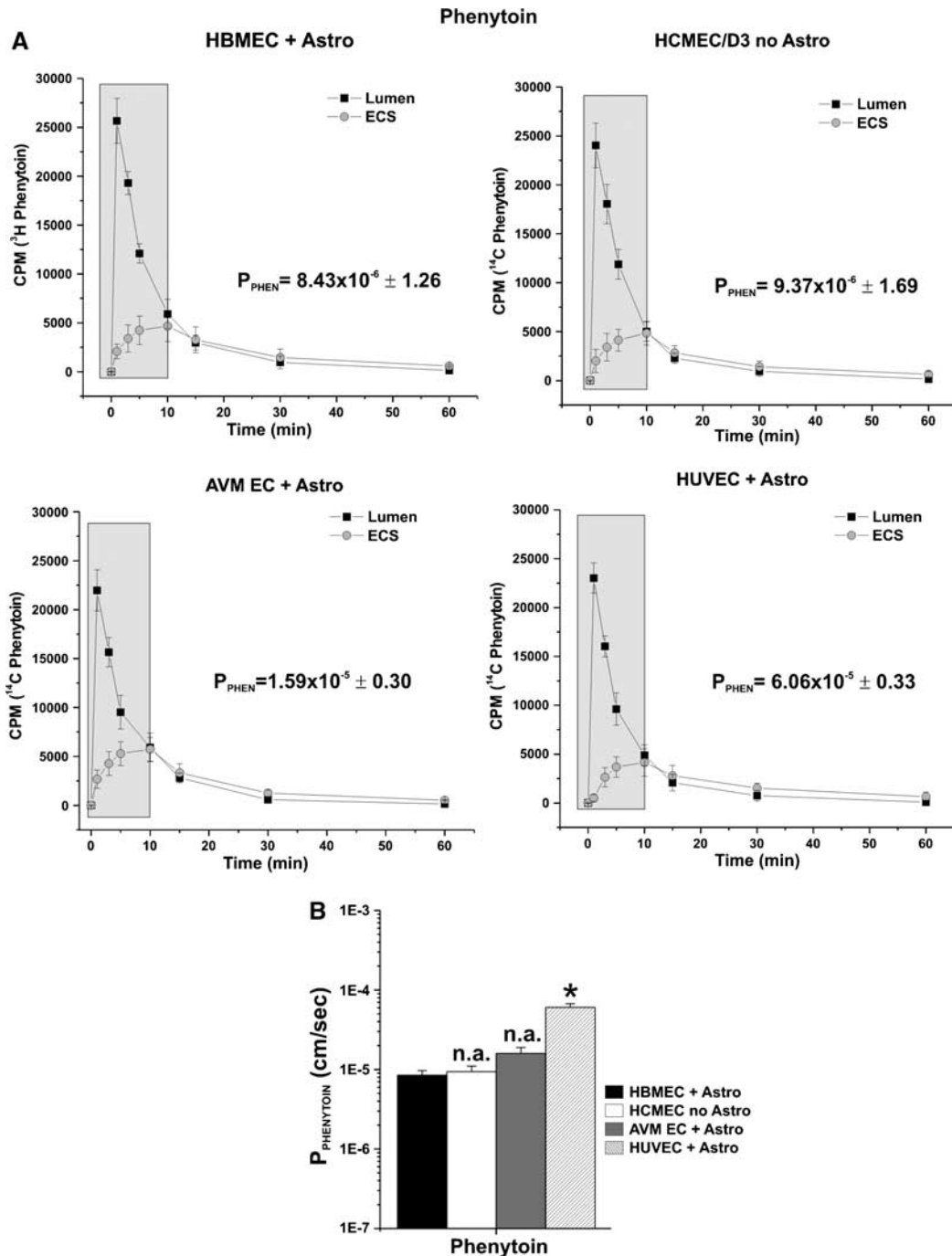


Figure 6 Phenytoin permeability. (A) Permeability measurements to [¹⁴C]phenytoin were also assessed in the DIV-BBB. (B) Note that the permeability values of phenytoin measured in HUVEC + HA models were significantly higher ($P < 0.05$) than AVM-EC, HBMEC + HA, or HCMEC/D3 setups. All experiments were performed in triplicate and permeability values are expressed in $\text{cm}/\text{sec} \pm \text{s.e.m.}$

(4) testing some of the new technologies that may facilitate controlled disruption of the tight junctions between endothelial cells. To these ends, the aim of this study was to assess the reliability of a model of the BBB utilizing a phenotypically normal, stable, immortalized human brain vascular endothelial cell line in comparison with primary endothelial cells. In this study, we have also outlined the importance

of organ specificity when selecting vascular endothelial cells to establish a BBB model that closely mimics the BBB *in vivo*. We demonstrated the advantages of the DIV-BBB over a conventional static culture system (Transwell). We have also assessed the effect of a commonly used anti-inflammatory drug to prevent BBB failure after flow cessation/reperfusion in the presence of circulating

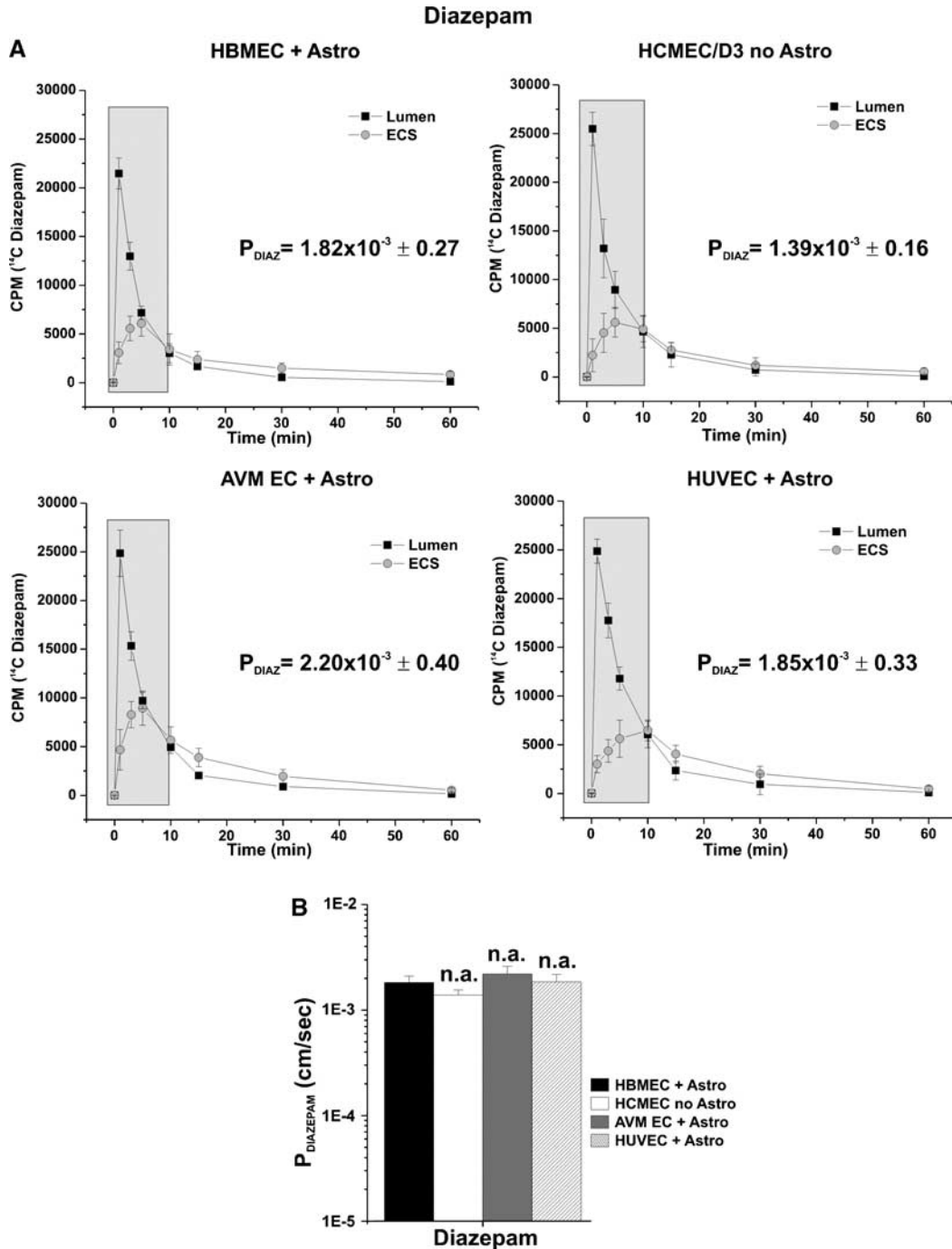


Figure 7 Permeability of diazepam. (A) By comparing the permeability values to [¹⁴C]diazepam, we find (B) no significant differences between HBMEC, HCMEC/D3, AVM-EC, or HUVEC setups ($\approx 2 \times 10^{-3}$). Permeability values are expressed in cm/sec \pm s.e.m. The asterisk * $P < 0.05$.

WBC, thus establishing a model to study the effect of inflammation at the BBB *in vitro*.

Role of Shear Stress in BBB Development and Cell Metabolism

Endothelial cells *in vivo* are long-lived cells continuously exposed to shear stress, a tangential force

generated by the flow of blood across their apical surfaces. Shear stress affects endothelial cell differentiation, tight junction formation, the expression of junction-related proteins (Arisaka *et al*, 1995; Yoshida *et al*, 1995), and induces mitotic arrest (Desai *et al*, 2002; Lin *et al*, 2000). An index of the endothelial ‘tightness’ of the monolayer is the TEER measured across the BBB (Santaguida *et al*, 2006). Our data clearly show that the exposure to flow, as found

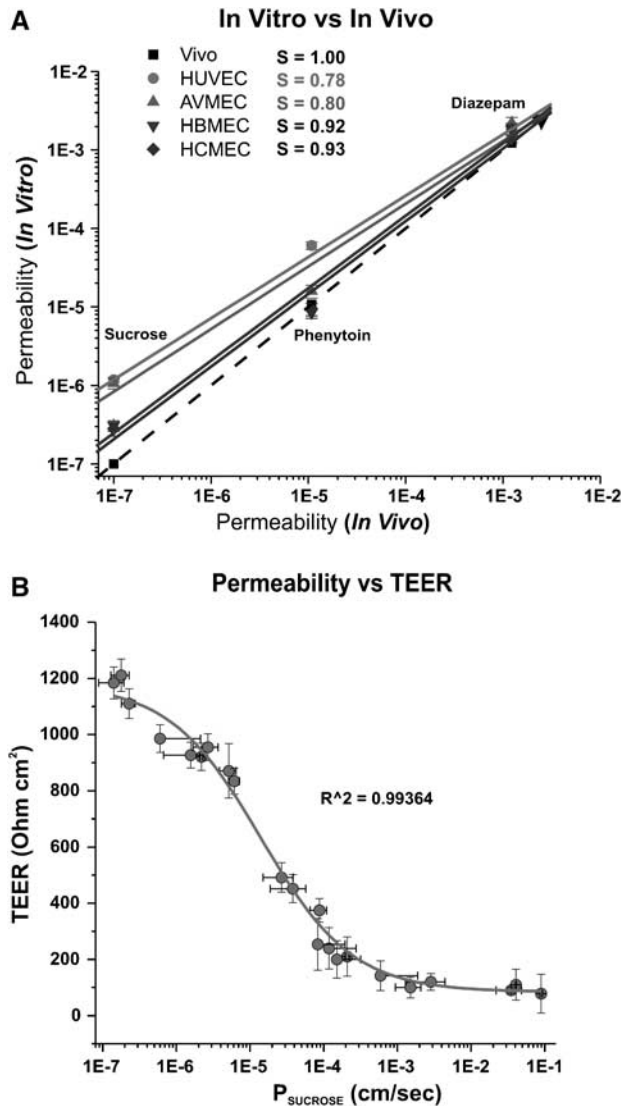


Figure 8 Correlation between permeability *in vivo* and *in vitro* in DIV-BBB system. **(A)** The dashed line indicates the idealized relationship if the data *in vivo* were identical to *in vitro* (slope (S) = 1). Note that permeability obtained in the DIV-BBB established with the use of HBMEC (S = 0.92) and HCMEC/D3 (S = 0.93) endothelial cells accurately reflects the *in vivo* scenario. AVM-EC (S = 0.80)- and HUVEC (S = 0.78)-based DIV-BBB resulted significantly less accurate especially to assess the permeability of polar compounds (such as sucrose). **(B)** The sigmoidal fit curve $y = A_2 + (A_1 - A_2) / (1 + (x/x_0)^p)$ describes the functional correlation between TEER values and permeability to the paracellular marker sucrose. Note that A1 represents the initial value (left horizontal asymptote), A2 is the final value (right horizontal asymptote), x0 is the center (point of inflection), and p (power) is the parameter that affects the slope of the area about the inflection point.

in vivo, allows endothelial cells cultured in the DIV-BBB flow apparatus (in the presence of abluminal glia) to achieve a TEER over 15-fold higher than in static conditions.

Of the different human endothelial cell types we tested (HBMEC, HUVEC, AVM, HCMEC/D3), only the immortalized human brain microvascular

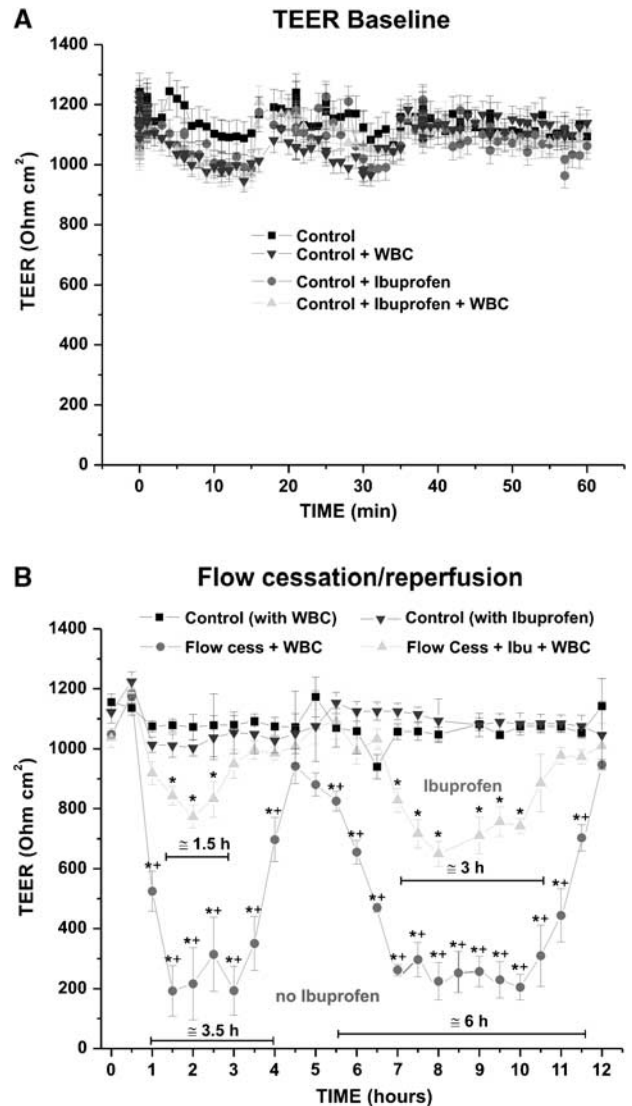


Figure 9 Functional assessment of the HCMEC/D3 *in vitro*-based BBB in an experiment of flow cessation/reperfusion with WBC. **(A)** TEER measurement in DIV-BBB modules established with the use of HCMEC/D3. No TEER differences were observed between the different experimental conditions and the controls. **(B)** Flow cessation/reperfusion caused a biphasic opening of the BBB. Pretreatment with ibuprofen partially prevented BBB failure and shortened the duration of the peak openings in comparison with the untreated modules. Note that all experiments were performed in triplicate. The asterisk ‘*’ indicates a significant difference (P < 0.05) from the controls, whereas ‘+’ indicates a significant (P < 0.05) difference between experimental flow cessation with and without ibuprofen.

endothelial cell line HCMEC/D3 was capable of achieving a high TEER in absence of abluminal glia. This suggests that (1) this newly developed cell line is capable of forming a very tight barrier and (2) the presence of abluminal glial for these cells is less determinant than the exposure to flow for the establishment of a functional BBB.

The assessment of glucose consumption/lactate production demonstrated that endothelial cells

grown in static conditions have an anaerobic metabolic pathway. By contrast, the same cells grown under dynamic conditions show a high propensity toward an aerobic type of metabolism (Santaguida *et al*, 2006). This observation is in

agreement with previous data demonstrating that exposure to shear stress induces metabolic changes (Desai *et al*, 2002) such as upregulation of the dehydrogenases and glyceraldehyde-3-phosphate dehydrogenase, and is accompanied by simultaneous decrease in enzymes of the NADH-depleting pathway, such as lactate dehydrogenase, which play key roles in the Krebs cycle. In addition to maintaining shear stress, the growth medium in the DIV-BBB is circulated in silicon tubing that allows for continuous exchange of oxygen and CO₂ with the external environment. Moreover, the gas-permeable tubing connecting the cartridge to the medium reservoir increases the exchange surface. In Transwell plates, these advantages for maintaining glucose and oxygen homeostasis are lost owing to lack of flow, and to limitation of the exchange surface by the size of the well.

Taking these two last points into account, our data also suggest that endothelial cells cultivated in the DIV-BBB are capable of adjusting their metabolic behavior to adapt to oxygen availability. Therefore, monitoring cellular metabolism is an important parameter in testing the adaptation of the endothelial cells chosen to establish a BBB *in vitro*. As shown by our data, the HCMEC/D3 cell line recapitulates the metabolic behavior of primary endothelial–glial co-cultures even in the absence of abluminal astrocytes.

Dynamic *In vitro* Blood Brain Barrier Mimics the BBB *In vivo*: Testing Clinical Protocols *In vitro*

Osmotic opening of the BBB by hyperosmotic mannitol solution is a common clinical procedure used to facilitate chemotherapeutic drug penetration into the brain parenchyma for the treatment of malignant brain tumors. The opening of the BBB is mediated by cerebrovascular dilatation, dehydration of endothelial cells, and contraction of their cytoskeleton, which leads to the widening of the inter-endothelial tight junctions. This mechanism is driven solely by the effect of the osmotic gradient of water from the inside to the outside of the cell body (Rapoport, 2000) and is fully reversible. Our experiments have shown that all of our DIV-BBB models (whether based on primary endothelial cell cultures or on the HCMEC/D3 endothelial cell line) closely mimic the *in vivo* BBB response to hyper-

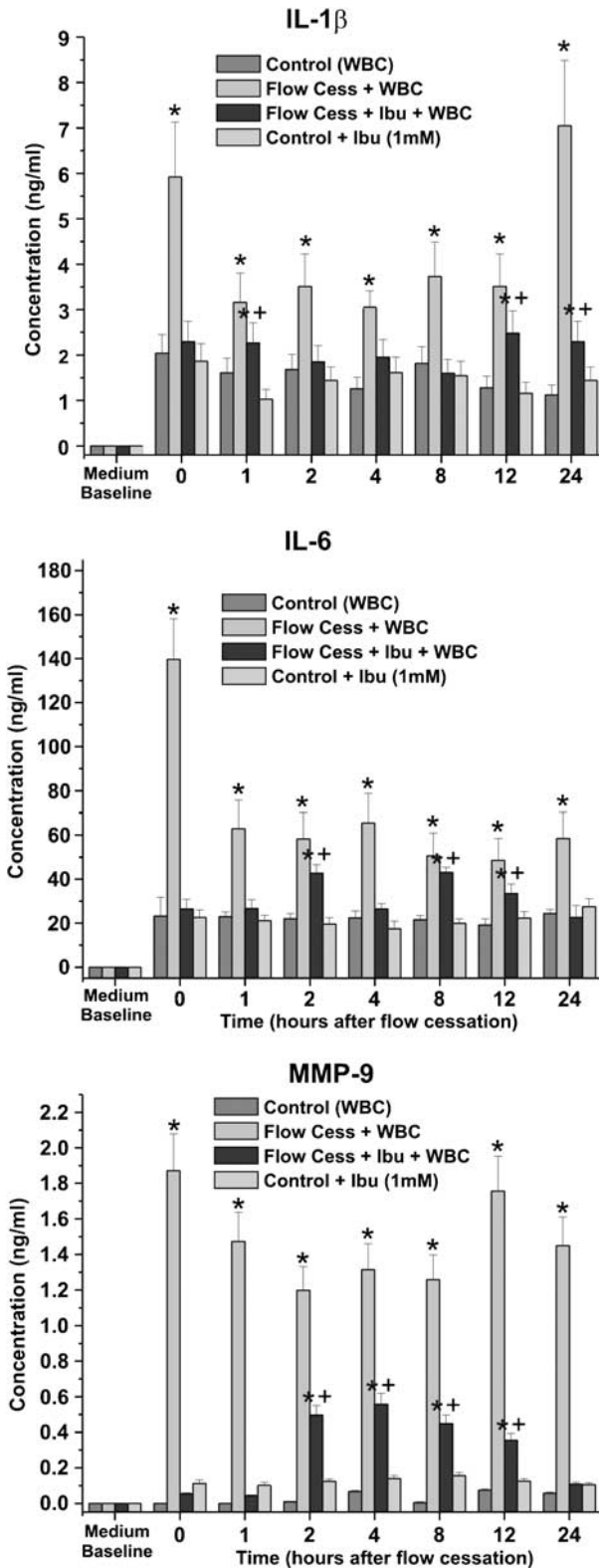


Figure 10 Measurement of proinflammatory cytokines IL-1 β , IL-6, and MCP-9. Levels of IL-1 β , IL-6, and MMP-9 were measured in medium samples in all experimental conditions. Note that pretreatment with ibuprofen significantly reduced the release of IL-1 β , IL-6, and MMP-9. These data are in agreement with the levels of BBB failure concomitantly assessed by TEER measurements. The asterisk '*' indicates a significant difference ($P < 0.05$) from the controls, whereas '+' indicates a significant ($P < 0.05$) difference between experimental flow cessation with and without ibuprofen.

osmolar mannitol (Figure 4). From this perspective, the use of the HCMEC/D3 cell line in conjunction with the DIV-BBB system offers significant advantages in comparison with primary cell cultures.

Pathophysiology of CNS Diseases: Assessing the Role of Inflammation in BBB Failure

Increasing evidence indicates that inflammation is involved in the pathogenesis of many neurological and neurodegenerative diseases and that the BBB dynamically responds to these inflammatory events. This is important because BBB failure can cause substances circulating in the blood that are normally excluded from the CNS (such as potassium, glutamate, and plasma proteins) to enter the brain, thus leading to a secondary process of CNS injury. For example, BBB failure after vasogenic brain trauma or focal brain ischemia may trigger the occurrence of status epilepticus (Karhunen *et al.*, 2005; Vezzani and Granata, 2005). Therefore, it seems reasonable to propose that the use of anti-inflammatory drugs (AIDs) may diminish the cumulative effects of inflammation in the brain. However, few AID clinical trials performed so far were minimal and equivocal in their outcomes. This likely occurred for several reasons, such as timing of AID administration, non-selective inhibition of cyclooxygenases (COX-1 and -2), inappropriate use of AIDs for a given disease or disease progression/severity or suboptimal dose in target sites. Given these considerations, the advantages that could come from the use of a reliable *in vitro* BBB model for the testing of AIDs are clearly evident.

For this instance, the DIV-BBB was successfully used to mimic an ischemic-like event *in vitro* in the presence of circulating WBC. The model was successfully used to assess the effect of ibuprofen, a well-known AID, to prevent BBB failure after normoxic flow cessation/reperfusion and activation of WBCs and vascular endothelium. Our results show that the ischemic-like insult simulated by flow cessation/reperfusion caused a biphasic opening of the BBB (Figure 7). However, in the DIV-BBB modules pretreated with 1 μ mol/L ibuprofen before flow cessation/reperfusion in the presence of WBC, the peak opening of the barrier is significantly lower and the intervals between the periods of opening is significantly shorter. These data strongly suggest that the inflammatory response that follows an ischemic-like event *in vivo* is the primary cause of BBB failure. This effect is relevant because BBB failure is related to the occurrence of secondary post-ischemic brain injuries.

Flow cessation/reperfusion triggered an inflammatory response that led to BBB failure as demonstrated by the biphasic decrease in TEER (Figure 9) observed during the course of the experiment. Additionally, BBB failure was paralleled by the intraluminal release (Figure 10) of proinflammatory

factors (IL-6 and IL-1 β) and MMP-9. Pretreatment with ibuprofen (0.125 mmol/L) prevented BBB failure by decreasing the inflammatory response after flow cessation/reperfusion.

Taken together, these results show that the DIV-BBB can find useful application in the evaluation of clinical procedures. A variety of clinical protocols and novel drugs for the treatment of CNS diseases could be reliably tested *in vitro* before moving to real-life applications.

Drug Delivery into the Central Nervous System: Dynamic *In vitro* Blood–Brain Barrier as a Tool to Assess Blood–Brain Barrier Permeability of Novel Drugs

Drug delivery to the CNS is subject to the permeability limitations imposed by the BBB. Several systems *in vitro* have been described to reproduce the physical and the biochemical behavior of an intact BBB, but most of these lack the key features of the barrier *in vivo*.

Permeability measurements of sucrose, phenytoin, and diazepam assessed in the DIV-BBB have shown that (1) the exposure to intraluminal flow plays an essential role in promoting BBB tightness; (2) the humanized DIV-BBB can successfully distinguish between permeability rankings of different classes of substances that penetrate the BBB by different mechanisms, thus providing reproducible results that can be reliably matched to the BBB *in situ*; (3) different from vascular endothelial primary cultures (Abbott, 2002; Hamm *et al.*, 2004), HCMEC/D3 cells grown under dynamic conditions differentiate into a very stringent BBB phenotype even without the presence of abluminal astrocytes. It is also important to note that despite the exposure to a quasi-physiological pulsatile flow and the presence of abluminal astrocytes, non-brain vascular endothelial cells (HUVECs) were the less capable to establish a BBB *in vitro* as stringent as the ones based on brain microvascular endothelial cells. This latter finding outlines the importance of organ specificity when selecting vascular endothelial cells to establish an *in vitro* BBB model.

What is Left to Transwell?

We have seen that static culture and co-culture models cannot reproduce the complete BBB *in vivo* despite having been used as relatively low cost tools for studying drug transport across the BBB. The attractive features of the Transwell model are its simplicity (easy to establish cultures) and the fixed volumes in each compartment that are useful for Michaelis–Menten kinetics of transport (Berezowski *et al.*, 2004). However, in the absence of shear stress, which plays a central role in the cerebrovascular system by promoting the differentiation and maintenance of the BBB phenotype, the endothelial cells

lose their 'BBB properties' (Desai *et al*, 2002; Santaguida *et al*, 2006). This greatly reduces the predictive accuracy of the permeability measurements of novel CNS drugs in Transwell plates.

Primary Human Endothelial Cell Cultures Versus Human Cell Lines

The use of human endothelial and glial cells isolated from human brain microvasculature can provide important advantages (e.g., improved accuracy of drug permeability values due to maintained substrate/transporter specificity) in the study of drug refractory brain disease, in prescreening and optimization of new drug formulations. However, ethical concerns as well as difficult availability clearly limit the use of endothelial and glial cells isolated from human brain tissue specimens. Not only are pure cultures of cells difficult to isolate technically from very small amounts of primary tissue, but also, once isolated, the cells cannot be stored for an extended period of time but have to be freshly re-isolated at short intervals from highly heterogeneous sources. These challenging obstacles can make the use of human brain-derived cells an unrealistic alternative for industrial purposes. However, under certain circumstances, such as studying particular brain diseases of different etiologies, the use of primary human brain-derived cultures still offers unique benefits that might outweigh the challenge of isolating and growing these cells.

In this study, we have reported significant progress in the effort of 'humanization' of the BBB model by the use of the HCMEC/D3 cell line that stably retains the morphological and functional characteristics of primary brain endothelial cells even in the absence of abluminal glial cells. The HCMEC/D3 cell line was previously demonstrated to grow indefinitely without phenotypic dedifferentiation, to be capable of expressing chemokine receptors, and to upregulate adhesion molecules in response to inflammatory cytokines. HCMEC/D3 cells also retain expression of multidrug resistance proteins (such as MDR1), which are commonly expressed in primary brain microvascular endothelial cells (Weksler *et al*, 2005).

Furthermore, permeability measurements of sucrose, phenytoin, and diazepam have shown that HCMEC/D3 cells cultured under flow conditions maintained *in vitro* physiological permeability properties of the BBB *in situ*. Other important biological parameters such as metabolic behaviors under static and dynamic conditions demonstrated a perfect correspondence with the other humanized DIV-BBB models tested. The same applies when HCMEC/D3 cells were used to evaluate BBB alterations in settings mimicking clinical protocols such as the osmotically driven opening of the BBB or the anti-inflammatory effect of an AID drug during flow cessation/reperfusion. To this end, the use of the

immortalized human brain microvessel endothelial cell line HCMEC/D3 could provide an appropriate, well-characterized, and cost-effective surrogate for primary brain vascular endothelial cells in many different applications, from drug delivery studies to screenings of novel therapeutic agents before clinical uses.

Summary

The DIV-BBB system in combination with primary human brain endothelial cells plus astrocytes, or with the HCMEC/D3 cell line in absence of astrocytes, can be successfully used to understand better the principles of brain drug delivery, to acquire relevant knowledge of the BBB physiology, and to study the mechanism of endothelial cell differentiation into a BBB phenotype. In addition, the DIV-BBB can be used to evaluate the consequences on BBB integrity of pathophysiological conditions and novel drug treatments.

References

- Abbott NJ (2002) Astrocyte-endothelial interactions and blood-brain barrier permeability. *J Anat* 200:629-38
- Antezana DF, Clatterbuck RE, Alkayed NJ, Murphy SJ, Anderson LG, Frazier J, Hurn PD, Traystman RJ, Tamargo RJ (2003) High-dose ibuprofen for reduction of striatal infarcts during middle cerebral artery occlusion in rats. *J Neurosurg* 98:860-6
- Arisaka T, Mitsumata M, Kawasumi M, Tohjima T, Hirose S, Yoshida Y (1995) Effects of shear stress on glycosaminoglycan synthesis in vascular endothelial cells. *Ann N Y Acad Sci* 748:543-54
- Banks WA, Ercal N, Price TO (2006) The blood-brain barrier in neuroAIDS. *Curr HIV Res* 4:259-66
- Berezowski V, Landry C, Lundquist S, Dehouck L, Cecchelli R, Dehouck MP, Fenart L (2004) Transport screening of drug cocktails through an *in vitro* blood-brain barrier: is it a good strategy for increasing the throughput of the discovery pipeline? *Pharm Res* 21:756-60
- Chen CH, Toung TJ, Sapirstein A, Bhardwaj A (2006) Effect of duration of osmotherapy on blood-brain barrier disruption and regional cerebral edema after experimental stroke. *J Cereb Blood Flow Metab* 26:951-8
- Cipolla MJ, Crete R, Vitullo L, Rix RD (2004) Transcellular transport as a mechanism of blood-brain barrier disruption during stroke. *Front Biosci* 9:777-85
- Cole DJ, Patel PM, Reynolds L, Drummond JC, Marcantonio S (1993) Temporary focal cerebral ischemia in spontaneously hypertensive rats: the effect of ibuprofen on infarct volume. *J Pharmacol Exp Ther* 266:1713-7
- Cucullo L, Hossain M, Rapp E, Manders T, Marchi N, Janigro D (2007) Development of a humanized *in vitro* blood-brain barrier model to screen for brain penetration of antiepileptic drugs. *Epilepsia* 48:505-16
- Cucullo L, McAllister MS, Kight K, Krizanac-Bengez L, Marroni M, Mayberg MR, Stanness KA, Janigro D (2002) A new dynamic *in vitro* model for the multi-

- dimensional study of astrocyte-endothelial cell interactions at the blood-brain barrier. *Brain Res* 951:243–54
- Davson H, Segal MB (1996) Blood-brain barrier. In: Davson H, Segal MB (eds), *Physiology of the CSF and Blood-Brain Barriers*. Boca Raton, FL: CRC, 49–91
- Desai SY, Marroni M, Cucullo L, Krizanac-Bengez L, Mayberg MR, Hossain MT, Grant GG, Janigro D (2002) Mechanisms of endothelial survival under shear stress. *Endothelium* 9:89–102
- Gasche Y, Soccal PM, Kanemitsu M, Copin JC (2006) Matrix metalloproteinases and diseases of the central nervous system with a special emphasis on ischemic brain. *Front Biosci* 11:1289–301
- Hamm S, Dehouck B, Kraus J, Wolburg-Buchholz K, Wolburg H, Risau W, Cecchelli R, Engelhardt B, Dehouck MP (2004) Astrocyte mediated modulation of blood-brain barrier permeability does not correlate with a loss of tight junction proteins from the cellular contacts. *Cell Tissue Res* 315:157–66
- Kalaria RN (1992) The blood-brain barrier and cerebral microcirculation in Alzheimer disease. *Cerebrovasc Brain Metab Rev* 4:226–60
- Karhunen H, Jolkkonen J, Sivenius J, Pitkanen A (2005) Epileptogenesis after experimental focal cerebral ischemia. *Neurochem Res* 30:1529–42
- Krizanac-Bengez L, Kapural M, Parkinson F, Cucullo L, Hossain M, Mayberg MR, Janigro D (2003) Effects of transient loss of shear stress on blood-brain barrier endothelium: role of nitric oxide and IL-6. *Brain Res* 977:239–46
- Krizanac-Bengez L, Mayberg MR, Cunningham E, Hossain M, Ponnampalam S, Parkinson FE, Janigro D (2006) Loss of shear stress induces leukocyte-mediated cytokine release and blood-brain barrier failure in dynamic *in vitro* blood-brain barrier model. *J Cell Physiol* 206:68–77
- Kubota H, Ishihara H, Langmann T, Schmitz G, Stieger B, Wieser HG, Yonekawa Y, Frei K (2006) Distribution and functional activity of P-glycoprotein and multidrug resistance-associated proteins in human brain microvascular endothelial cells in hippocampal sclerosis. *Epilepsy Res* 68:213–28
- Latour LL, Kang DW, Ezzeddine MA, Chalela JA, Warach S (2004) Early blood-brain barrier disruption in human focal brain ischemia. *Ann Neurol* 56:468–77
- Lee SW, Kim WJ, Park JA, Choi YK, Kwon YW, Kim KW (2006) Blood-brain barrier interfaces and brain tumors. *Arch Pharm Res* 29:265–75
- Levis KA, Lane ME, Corrigan OI (2003) Effect of buffer media composition on the solubility and effective permeability coefficient of ibuprofen. *Int J Pharm* 253:49–59
- Lin K, Hsu PP, Chen BP, Yuan S, Usami S, Shyy JY, Li YS, Chien S (2000) Molecular mechanism of endothelial growth arrest by laminar shear stress. *Proc Natl Acad Sci USA* 97:9385–9
- Lorberboym M, Blankenberg FG, Sadeh M, Lampl Y (2006) *In vivo* imaging of apoptosis in patients with acute stroke: correlation with blood-brain barrier permeability. *Brain Res* 1103:13–9
- Mashour GA, Boock RJ (1999) Effects of shear stress on nitric oxide levels of human cerebral endothelial cells cultured in an artificial capillary system. *Brain Res* 842:233–8
- Minagar A, Alexander JS (2003) Blood-brain barrier disruption in multiple sclerosis. *Mult Scler* 9:540–9
- Pardridge WM (2005) The blood-brain barrier: bottleneck in brain drug development. *NeuroRx* 2:3–14
- Parkinson FE, Friesen J, Krizanac-Bengez L, Janigro D (2003) Use of a three-dimensional *in vitro* model of the rat blood-brain barrier to assay nucleoside efflux from brain. *Brain Res* 980:233–41
- Rapoport SI (2000) Osmotic opening of the blood-brain barrier: principles, mechanism, and therapeutic applications. *Cell Mol Neurobiol* 20:217–30
- Santaguida S, Janigro D, Hossain M, Oby E, Rapp E, Cucullo L (2006) Side by side comparison between dynamic versus static models of blood-brain barrier *in vitro*: A permeability study. *Brain Res* 1109:1–13
- Shigemori Y, Katayama Y, Mori T, Maeda T, Kawamata T (2006) Matrix metalloproteinase-9 is associated with blood-brain barrier opening and brain edema formation after cortical contusion in rats. *Acta Neurochir Suppl* 96:130–3
- Stamatovic SM, Dimitrijevic OB, Keep RF, Andjelkovic AV (2006) Inflammation and brain edema: new insights into the role of chemokines and their receptors. *Acta Neurochir Suppl* 96:444–50
- Stanness KA, Westrum LE, Fornaciari E, Mascagni P, Nelson JA, Stenglein SG, Myers T, Janigro D (1997) Morphological and functional characterization of an *in vitro* blood-brain barrier model. *Brain Res* 771:329–42
- Unterberg AW, Stover J, Kress B, Kiening KL (2004) Edema and brain trauma. *Neuroscience* 129:1021–9
- van der FM, Hoppenreijns S, van Rensburg AJ, Ruyken M, Kolk AH, Springer P, Hoepelman AI, Geelen SP, Kimpen JL, Schoeman JF (2004) Vascular endothelial growth factor and blood-brain barrier disruption in tuberculous meningitis. *Pediatr Infect Dis J* 23:608–613
- Vezzani A, Granata T (2005) Brain inflammation in epilepsy: experimental and clinical evidence. *Epilepsia* 46:1724–43
- Walker MC, Alavijeh MS, Shorvon SD, Patsalos PN (1996) Microdialysis study of the neuropharmacokinetics of phenytoin in rat hippocampus and frontal cortex. *Epilepsia* 37:421–7
- Wekslar BB, Subileau EA, Couraud PO (2005) Blood-brain barrier-specific properties of a human adult brain endothelial cell line. *FASEB J* 19:1872–4
- Yoshida Y, Okano M, Wang S, Kobayashi M, Kawasumi M, Hagiwara H, Mitsumata M (1995) Hemodynamic-force-induced difference of interendothelial junctional complexes. *Ann N Y Acad Sci* 748:104–20